

First-principles phonon calculations of thermal expansion path of Fe₂Mo Laves phase

Dmitry Vasilyev

Baikov Institute of Metallurgy and Materials Science of RAS, 119334, Moscow, Leninsky Prospekt 49, Russia

dvasilyev@imet.ac.ru ; vasilyev-d@yandex.ru

Abstract. Precipitation of the topologically close-packed Fe₂Mo Laves phase at the interface between the nuclear fuel and the fuel element cladding can significantly weaken the strength characteristics of the cladding and fuel. Despite the importance of designing materials for the cladding of fuel rods, the thermodynamic properties and the trajectory of the thermal expansion path of the Fe₂Mo remain poorly understood. The thermodynamic properties of the Fe₂Mo have been studied using the finite-temperature quantum mechanical calculations within the frame of the density functional theory (DFT) under the quasiharmonic approximation. The vibrational contribution to the free energy was obtained using phonon calculations. The thermal expansion path of Fe₂Mo was predicted by comparing between free energies calculated in different directions. A path with the least energy was chosen as the trajectory of thermal expansion. The obtained result was compared with the path calculated in previous theoretical work used the Debye – Grüneisen approach and accounted magnetic subsystem to calculate the vibrational and magnetic contributions to the free energy. This comparison reveals that these two approaches are in good agreement with each other. The work shows that the Fe₂Mo possesses a non-isotropic thermal expansion. The heat capacity and volumetric expansion at constant pressure are modelled. The calculated results analyzed and are in satisfactory agreement with the experimental data. Obtained results can be useful for further design of fuel element cladding materials intended for generation IV reactors, the operating temperature of which should be above 873 K.

Keywords: Laves phase; First-principles calculations; Phonon calculations; Debye-Grüneisen model; Thermal expansion path; Thermodynamic properties

1. Introduction

The Laves phase Fe₂Mo is an intermetallic compound that can be precipitated from solid solutions as a result of product operation at high temperatures and under irradiation conditions. On the one hand, the Fe₂Mo is considered to be a useful hardening phase, since its precipitation from the solid solution of structural steels can improve toughness, creep and oxidation resistance [1]. On the other hand, a loss of toughness of ferritic-martensitic steels is directly related to the precipitation of the Fe₂Mo [2], and the precipitation of Fe₂Mo at the interface between the fuel element cladding and nuclear fuel can cause deterioration of their mechanical properties [3].

Fe₂Mo belongs to the Fe-Mo system, which is one of the basic binary phase diagrams used to design ferritic steels.

Ferritic steels are promising candidates for creating materials that are planned to be used in the production of fuel rods and vessel claddings for nuclear reactors of the IV generation, and the first wall in fusion reactors [4], this is due to their good resistance to swelling and creep caused by irradiation, good thermal conductivity and low coefficient of thermal expansion [5, 6].

The precipitation of Fe₂Mo leads to the depletion of the steel matrix in such strengthening elements as Mo or W [7]. For example, a large precipitation of Fe₂Mo in the HT9 matrix leads to a deterioration in the mechanical properties of the fuel element cladding [3].

The lattice parameters of Fe₂Mo were theoretically calculated in [8, 9, 10, 11] using Density Functional Theory (DFT) at T = 0 K. Experimental values of Fe₂Mo parameters obtained at 1073 K were reported in [10, 12, 13].

As far as is known, the thermodynamic properties of Fe₂Mo remain poorly understood. The thermal expansion path of Fe₂Mo was calculated in [14] using first-principles calculations with applying the quasi-harmonic Debye–Grüneisen (QDG) approximation and taking into account the magnetic entropy to calculate the vibrational and magnetic contributions to the free energy.

In the presented work, calculations of the free energies of Fe₂Mo carried out for different directions of thermal expansions were performed using DFT-based quasi-harmonic phonon approach. Comparison of the calculation results obtained in this work with the results reported in [14], where QDG method was used, shows that these results are in good agreement with each other.

Finally, the thermal expansion $V(T)$, heat capacity $C_p(T)$ of Fe₂Mo were calculated along the thermal expansion path. The results can be used to construct Gibbs potentials for phase diagram calculations, as well as to obtain properties whose experimental evaluation can be difficult.

2. Theory and Methods

Under the quasi-harmonic approximation, the Helmholtz free energy $F(V, T)$ takes the form according to [15-17]

$$F(V, T) = E_{tot}(V) + F_{el}(V, T) + F_{vib}(V, T) + F_{mag}(V, T) - TS_{conf} \quad (1)$$

where $E_{tot}(V)$ is the static total energy at T = 0 K. $F_{el}(V, T)$, $F_{vib}(V, T)$, $F_{mag}(V, T)$ are the electronic, vibrational and magnetic free energies contributions. S_{conf} is the ideal configurational entropy.

2.1. Electronic energy

The contribution from the thermal electron excitation $F_{el}(V, T)$ to the free energy was computed as expressed in [18]

$$F_{el}(V, T) = E_{el}(V, T) - TS_{el}(V, T), \quad (2)$$

with E_{el} is given by [19, 20]

$$E_{el}(T, V) = N_A \int_{-\infty}^{\infty} n(\varepsilon, V) f(\varepsilon, T) \varepsilon d\varepsilon - N_A \int_{-\infty}^{\varepsilon_F} n(\varepsilon, V) \varepsilon d\varepsilon \quad (3)$$

where $n(\varepsilon, V)$ is the total electronic density of states (e-DOS), $f(\varepsilon, T)$ is the Fermi-Dirac distribution and N_A is Avogadro constant. Where the electronic entropy S_{el} takes the form

$$S_{el}(T, V) = N_A \int_{-\infty}^{\infty} n(\varepsilon, V) (f(\varepsilon, T) \ln f(\varepsilon, T) + (1 - f(\varepsilon, T)) \ln(1 - f(\varepsilon, T))) d\varepsilon \quad (4)$$

2.2. Vibrational energy

The vibration free energy $F_{vib}(V, T)$ was calculated from phonon density of states (PDOS) as formulated in [21, 22]

$$F_{vib}(V, T) = k_B T \int_0^{\infty} \ln \left[2 \cdot \sinh \frac{\hbar \omega}{2k_B T} \right] g(\omega, V) d\omega \quad (5)$$

where \hbar and k_B are the reduced Planck and Boltzmann constants respectively, $g(\omega, V)$ represents PDOS as a function of phonon frequency ω calculated at volume V .

2.3. Magnetic energy

In order to take into account, the magnetic phase transition of Fe₂Mo Laves phase the Hillert - Jarl model described in [24] was used. According to this model the magnetic energy is expressed as

$$F'_{mag}(T) = RT \ln(\beta + 1) f(\tau) \quad (6)$$

where $\tau = T/T_c$; T_c and β are the Curie temperature and the average magnetic moment of a compound, the $f(\tau)$ is defined in [24].

Due to the fact that the magnetic internal energy is already taken into account in the DFT calculations of the total energy, the magnetic energy $F_{mag}(V, T)$ contribution to the free energy of the compound was calculated using the following expression

$$F_{mag}(V, T) = F'_{mag}(T) - F'_{mag}(0K) \quad (7)$$

The configurational entropy S_{conf} was treated by the mean-field approximation

$$S_{conf} = N_A k_B \sum_{i=1}^n c_i \ln c_i \quad (8)$$

where c_i is atomic concentrations.

2.4. First-principles calculations

The calculations were carried out using the FP-LAPW method, as implemented in the WIEN2k code [25]. The exchange–correlation interaction was treated using the generalized gradient approximation (GGA) by Perdew, Burke, and Ernzerhof (PBE) potential [26]. The first irreducible Brillouin zones of the unit cells were sampled by a 13 x 13 x 6 k -point mesh by employing the Monkhorst-Pack scheme [27]. The energy convergence criterion of electronic self-consistency was set to 10⁻⁸ eV/atom.

The vibrational energy was calculated from phonon spectra, which obtained through lattice dynamical simulations performed using Phonopy package [23], where a method of small atom displacements is used to calculate forces affecting the atoms. The size of a Fe₂Mo supercell used in the present calculation is 2 × 2 × 1. To model the Brillouin zone for calculating the forces, the 4 × 4 × 4 Monkhorst–Pack mesh [27] was used.

3. Results and discussion.

3.1. Ground state properties

3.1.1. Phase stability of Fe_2Mo

The Fe_2Mo Laves phase is a stoichiometric compound with the C14 structure type and the space group $P6_3/mmc$ with No. 194 and with the $hP12$ Pearson symbol. The Fe_2Mo lattice is schematically shown in Figure 1.

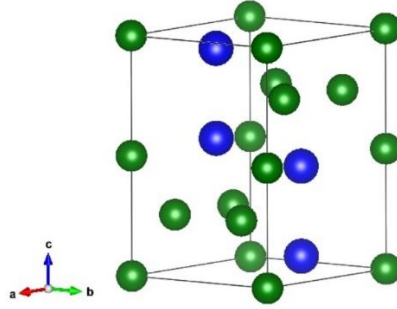


Figure 1. Scheme of the crystal lattice of Fe_2Mo Laves phase, green circles represent Fe atoms and blue circles represent Mo atoms.

All computations in this work were performed using spin-polarized calculations. The lattice parameters of Fe_2Mo were obtained using structural relaxation procedure. The calculated lattice parameters of Fe_2Mo are given in Table 1 and Figure 2, the experimental values of parameters taken in [10, 12, 13] and theoretical data [8-10, 14] are shown here too. The lattice parameters of Fe_2Mo calculated in this work using DFT at $T = 0$ K are $a = 8.829$ and $c = 14.693$ bohr, which is very close to the result obtained in [8] with $a = 8.823$ and $c = 14.727$ bohr.

Table 1

Lattice parameters of Fe_2Mo obtained in this work in comparison with the theoretical and experimental data reported in other works.

	a (bohr)	c (bohr)	c/a	V (bohr ³)
This work	8.829	14.693	1.664	991.822
Exp. [10]	8.967	14.615	1.630	1017.664
Exp. [13]	8.938	14.589	1.632	1009.409
Exp. [12] ^a	8.940	14.679	1.642	1016.115
This work ^b	8.982	14.585	1.624	1018.986
Calc. [14] ^c	8.995	14.577	1.621	1021.460
Calc. [8]	8.823	14.727	1.669	992.842
Calc. [9]	8.804	14.632	1.662	982.251
Calc. [10]	8.848	14.286	1.615	968.528

^a Obtained at $T = 1073$ K after 1500 hours of thermal treatment.

^b Calculated at $T = 1073$ K in this work using DFT-based phonon calculation.

^c Calculated in [14] at $T = 1073$ K using QDG approach and magnetic entropy.

3.1.2 Calculation outline

In order to investigate thermal expansion paths of Fe_2Mo Laves phase the numbers of possible thermal expansion trajectories were considered. Four selected trajectories (path) of Fe_2Mo thermal expansion are shown in Figure 2, as an example. All these paths intersect in the point with the (a_0, c_0) coordinates, these are the equilibrium lattice parameters of Fe_2Mo calculated at ground state, which listed in Table 1. Along the $n0$ path the $c/a = 1.664$ ratio remains constant, this is the trajectory of isotropic thermal expansion. The $n1$ path is passing through the experimental data [12] obtained at $T = 1073$ K after 1500 hours of annealing treatment, which shown in Figure 2 by the blue triangle. The trajectory $n2$ passes through the coordinates of the lattice parameters obtained experimentally in [13], which are shown by the red triangle. The free energies calculated by (1) were obtained along each ni path and compared between themselves. Then, the trajectory with the least free energy was chosen as the path of thermal expansion of Fe_2Mo .

This calculation scheme is similar to a search of thermal expansion path (STEP) outlined in [14], but in this work the vibrational free energy was obtained using phonon dispersion curves calculated along each ni path. The main motivation to carry out the present work was to compare the obtained results with results calculated in [14], where the Debye–Grüneisen approach and magnetic entropy were used.

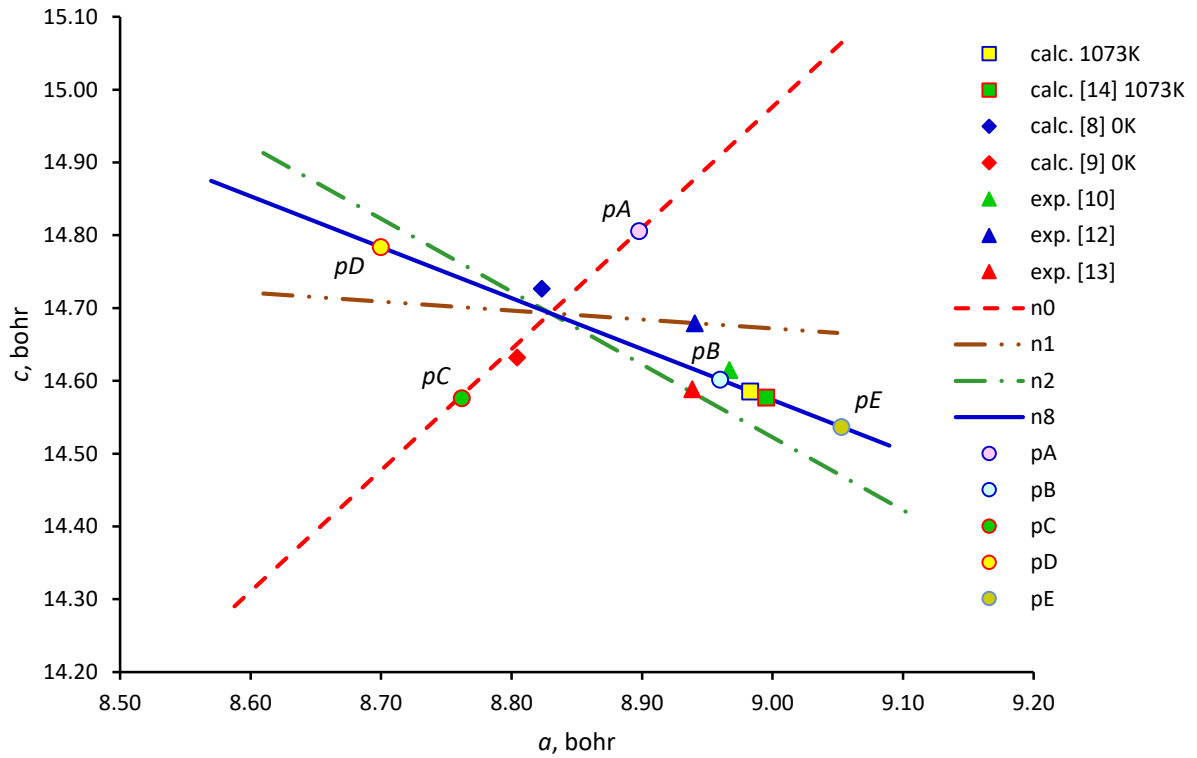


Figure 2. The outline of calculations. The intersection point of the $n0$, $n1$, $n2$, and $n8$ paths corresponds to the lattice parameters (a_0, c_0) of Fe_2Mo calculated in this work using DFT at the ground state. The theoretical data of lattice parameters calculated in [8, 9] with DFT at $T = 0$ K are shown by blue and red diamonds. The experimental parameters obtained at $T = 1073$ K in [10, 12, 13] are shown by the blue, green and red triangles. The lattice parameters of Fe_2Mo calculated in this work using DFT-based phonon method and obtained in [14] at $T = 1073$ K by applying the quasi-harmonic Debye - Grüneisen approach and magnetic entropy are shown by the yellow and the green squares, respectively. The description of the pA , pB , pC , pD and pE points is in the text.

3.1.3 Calculations of electronic and phonon density of states

The vibrational free energies $F_{vib}(T)$ calculated by (5) make the main contribution to the Helmholtz free energy (1). The phonon dispersion curves and the corresponding phonon density of states (PDOS), shown in Figure 3, were calculated at selected points on the coordinate plane (a, c) presented in Figure 2. Figure 3 (f) plots the results obtained at the point with the lattice parameters (a_0, c_0) of Fe_2Mo calculated in this work which associated with the $T = 0$ K. Figure 3 (a) plots the results obtained at the point pA which lies on the $n0$ path, as shown in Figure 2. The other results of the phonon calculations obtained at the pB , pC and pD points are shown in Figure 3 (b), Figure 3 (c) and Figure 3 (d), respectively. The positive phonon frequencies reveal the dynamical stability of the Fe_2Mo with these lattice parameters.

While, the phonon dispersions and density of states of Fe_2Mo calculated at point pE which is on the $n8$ path, as shown in Figure 3 (e), display extensive imaginary phonon modes, which means that at the pE the Fe_2Mo becomes unstable if the lattice parameters reach these values at heating. The calculation predicts that point pE corresponds to $T = 1291$ K.

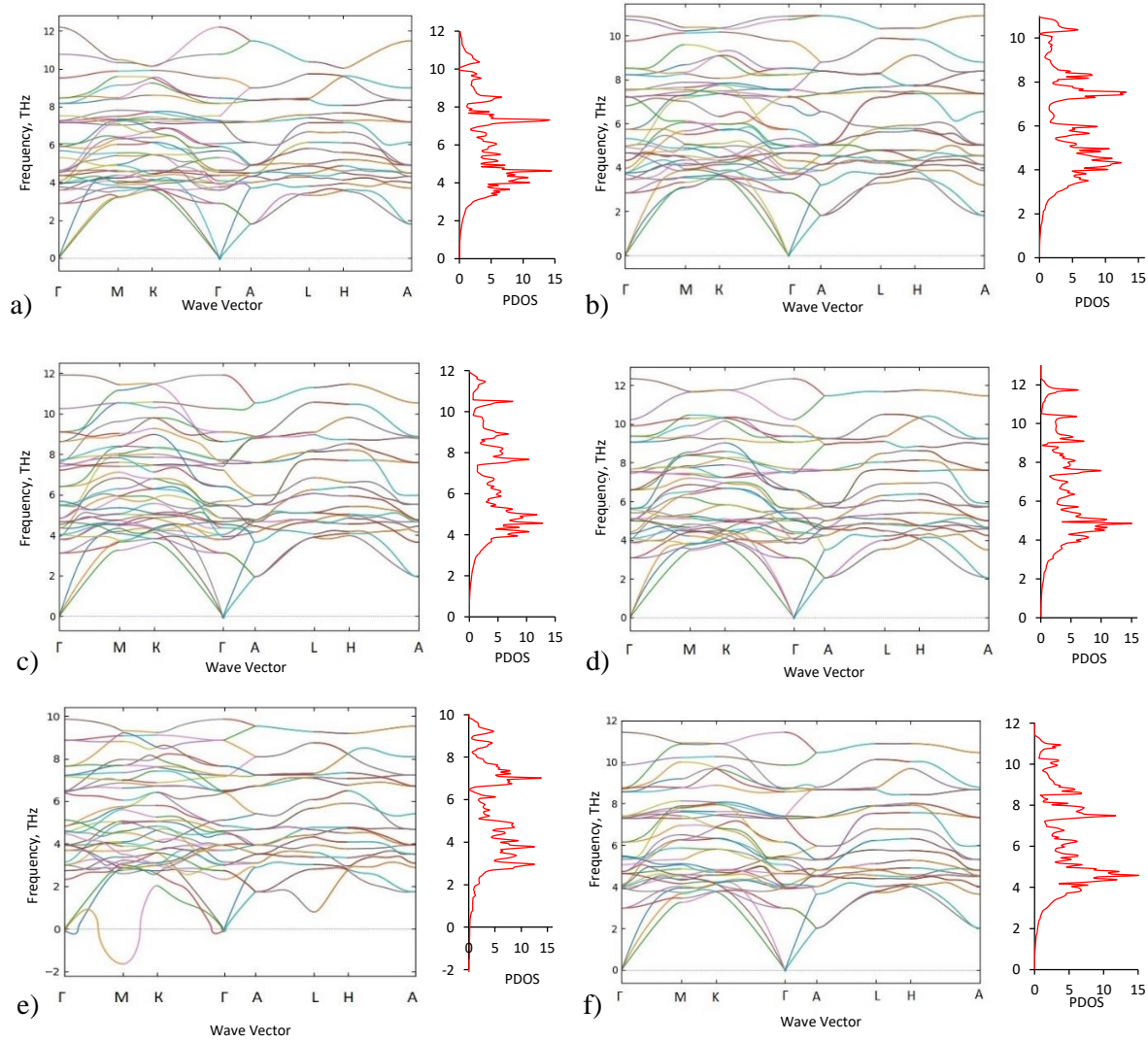


Figure 3. The phonon dispersion curves and the phonon density of states (PDOS) for Fe_2Mo Laves phases calculated at a) point pA ; b) point pB ; c) point pC ; d) point pD ; e) point pE ; f) point (a_0, c_0) .

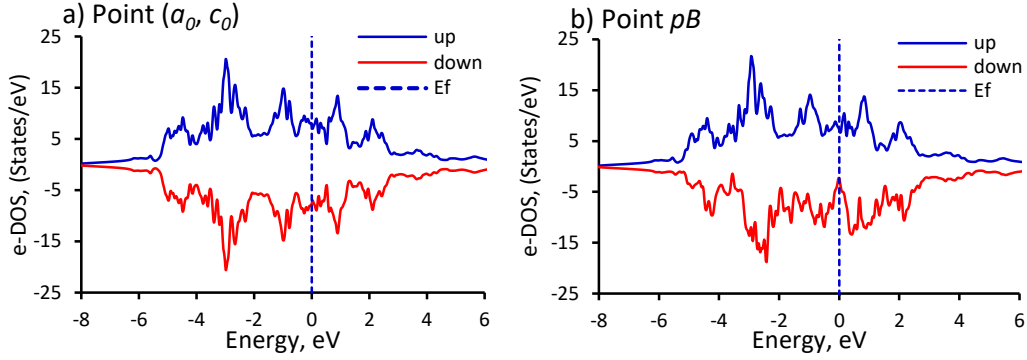


Figure 4. Total electron density of states (e-DOS) for Fe_2Mo Laves phases calculated a) at point (a_0, c_0) and b) at point pB .

The electron energies (2) were calculated along all ni directions, shown in Figure 2, through electron densities, according to (3) and (4). An example of such calculations, that is the total electronic density of states (e-DOS) of Fe_2Mo calculated at points (a_0, c_0) and pB are shown in Figure 4 (a) and Figure 4 (b), respectively.

3.2. Compound stability at finite temperatures

3.2.1. Calculations of free energies

All the energy contributions to the Helmholtz free energy of Fe_2Mo , namely, total, electronic (2), vibrational (5) and magnetic (7) energies were calculated along each ni path selected in Figure 2. Then, for each ni path the free energy $F(V, T)$ of Fe_2Mo was obtained according (1) as a sum of these energy parts. Figure 5 demonstrates an example of the free energy $F(V, T)$ obtained along $n8$ path, calculated at different temperatures and volumes. The total energy calculated at $T = 0$ K and equilibrium volumes V_0 , which were obtained at the minimum of thermodynamic functions, are shown in Figure 5 by the red dashed and blue dotted lines, respectively. The thermal expansion can be seen as an increase in the equilibrium volume shown in Figure 5.

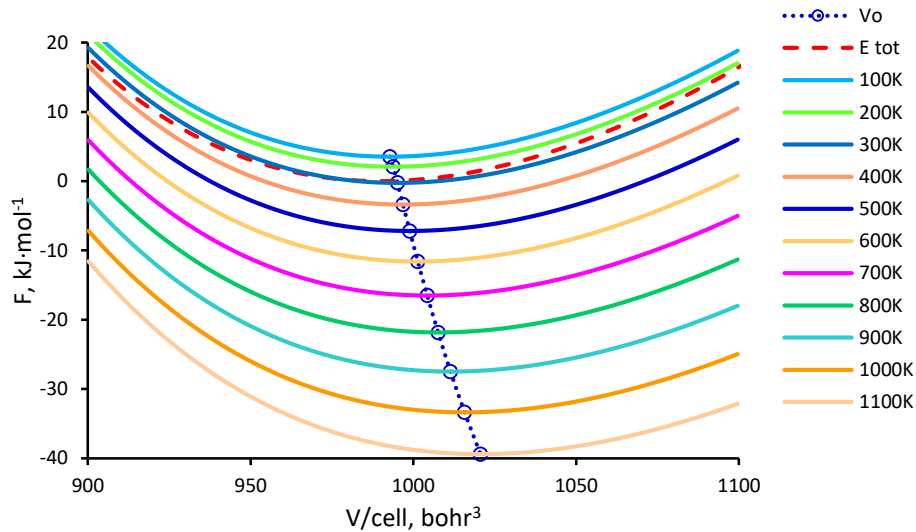


Figure 5. The free energy curves $F(V, T)$ of Fe_2Mo calculated at different temperatures for the $n8$ path. The equilibrium volumes $V_0(T)$ are shown by the blue dotted line. The red dashed line represents the total energy $E_{tot}(V)$.

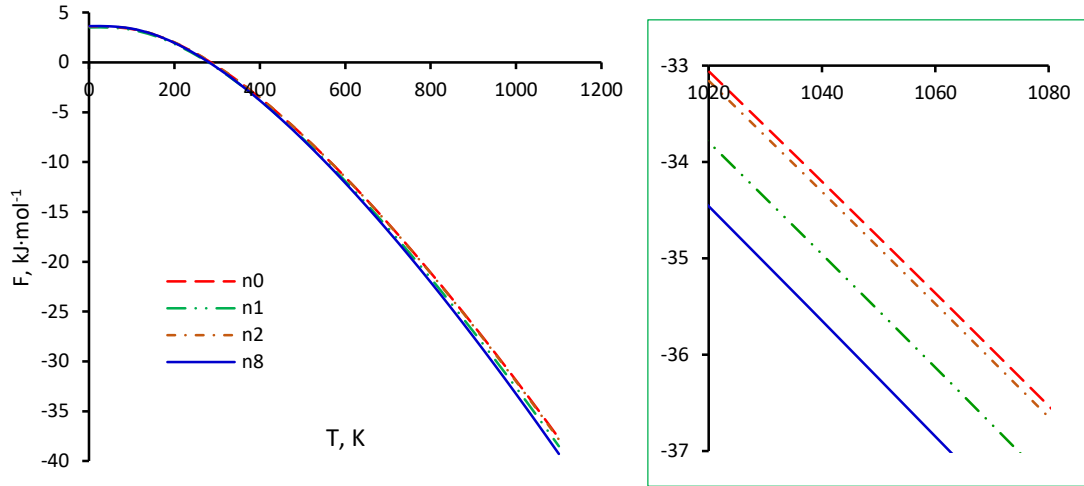


Figure 6. The free energy curves $F(T)$ of Fe_2Mo calculated along $n0$, $n1$, $n2$ and $n8$ paths, using first-principles phonon calculation. In the box on the right, the magnified values are given for convenience.

The free energies $F(V_0, T)$ calculated by (1) at corresponding equilibrium volumes along $n0$, $n1$, $n2$ and $n8$ paths are shown in Figure 6. According to this calculation the $n8$ possess the lowest energy among the other paths. Thus, $n8$ is the path of thermal expansion of Fe_2Mo .

The free energy of Fe_2Mo calculated by (1) using DFT-based phonon calculations obtained for the thermal expansion path $n8$ is shown in Figure 7 by the solid blue line. For the sake of comparison, the free energy of Fe_2Mo calculated using QDG approach and magnetic entropy [14] is shown in Figure 7 by the red dashed line.

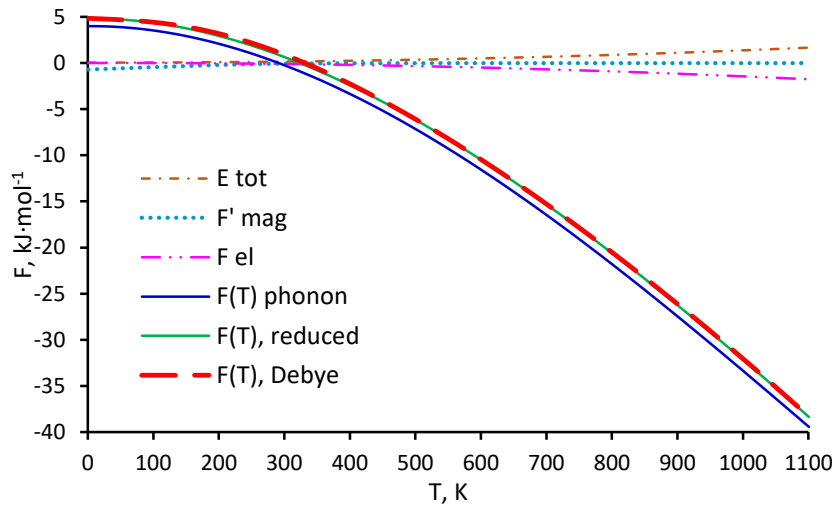


Figure 7. The free energy ($F(T)$, *phonon*) obtained as a sum of the total, electronic, magnetic and vibrational energy calculated using first-principles phonon calculation along the thermal expansion path of Fe_2Mo shown in comparison together with the free energy ($F(T)$, *Debye*) calculated using quasi-harmonic Debye - Grüneisen approximation reported in [14] and the free energy ($F(T)$, *reduced*) reduced to the zero-point energy expressed within the Debye model.

The total energy, electronic (2) and magnetic (7) energies contributing to the free energy of Fe_2Mo , are also shown in Figure 7.

Since the Debye model assumes the presence of zero vibrations [15], so if we bring the free energy calculated using phonons to the energy calculated using the Debye model, then we get the reduced function shown in Figure 7 by the solid green line.

The results presented in Figure 7 show that the free energy calculated in [14] using QDG closely match with the reduced free energy obtained using DFT-based phonon approach implemented in this work.

The $n8$ path of thermal expansion of Fe_2Mo which is the most energetically favorable among the other paths as follow from the calculations shown in Figure 6, is completely coincides with the path calculated in [14] using QDG approach and magnetic entropy.

3.2.2. Thermodynamic properties of Fe_2Mo

Thermodynamic properties were calculated along the most energetically stable thermal expansion path of Fe_2Mo . The calculated volume expansion $V(T)$ of Fe_2Mo is shown in Figure 8 (a) together with experimental data [10, 12, 13] and the theoretical calculation [14] for comparison.

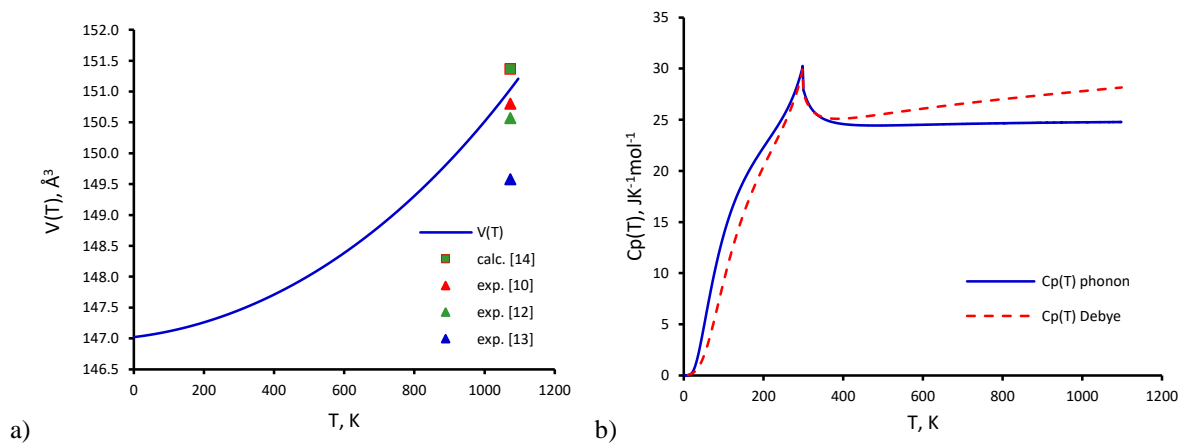


Figure 8. a) The volume expansion $V(T)$ (in Å^3) calculated using first-principles phonon calculation along the thermal expansion path of Fe_2Mo Laves phase in comparison with the experimental data [10, 12, 13] shown by the red, green and blue triangles; and the lattice parameters of Fe_2Mo calculated in [14] using the quasi-harmonic Debye - Grüneisen approach is shown by the green square. b) The isobaric heat capacities $C_p(T)$ obtained using the first-principles based phonon approach and the Debye - Grüneisen model calculated along the thermal expansion path of Fe_2Mo . The kink is a ferro/paramagnetic phase transition predicted by used the model [24].

The isobaric heat capacity $C_p(T)$ calculated along the thermal expansion path of Fe_2Mo using DFT-based phonon and QDG approaches are plotted in Figure 8 (b) by the blue solid line and the red dashed line, a kink at 299 K [14] corresponds to the ferro/paramagnetic phase transition as the applied model [24] predicts.

As far as is known, there aren't any available experimental data on the ferro/paramagnetic phase transition temperature for Fe_2Mo , so a study of an accurate value of the Curie temperature is still necessary.

3.2.3. Discussion

In order to predict a trajectory of the thermal expansion path of Fe₂Mo the free energies were calculated along different directions intersected at the point (a_0, b_0), which is associated with T = 0 K. The selected four paths $n0$, $n1$, $n2$ and $n8$ are shown in Figure 2. The phonon dispersion curves and their correspondent density of states calculated along the $n8$ path at the pD , (a_0, c_0), pB and pE points are shown in Figure 3 (d), Figure 3 (f), Figure 3 (b) and Figure 3 (e), respectively.

This order reflects the change in vibration energy from compression, which is at point pD , to expansion, which is at point pE , which corresponds to T = 1291 K, as predicted by the current calculation. At this temperature Fe₂Mo becomes unstable according to the Fe – Mo phase diagram estimated by Massalski et al. [28]. According to the diagram, at 1200 K in equilibrium, this compound undergoes a phase transformation and decomposes into a body-centered cubic (bcc) solid solution and a μ - phase. Thus, the imaginary phonon modes shown in Figure 3 (e), confirm that at this temperature the Fe₂Mo become an unstable compound indeed.

These figures reveal that with an increase in temperature during expansion along the $n8$ path, the vibrational frequencies slightly decrease. This relatively slight frequencies softening with temperature implies that the Fe₂Mo can possess heat-resistant properties.

An analysis of the isotropic expansion along the $n0$ path shown in Figure 3 (c), Figure 3 (f) and Figure 3 (a) reveals that with the increasing volume, the vibrational frequencies change insignificantly. Apparently, it can reflect the fact that this direction of thermal expansion is not an energetically favorable.

The graph of volume expansion of Fe₂Mo shown in Figure 8 (a) reveals that the values of lattice parameters calculated in this work at 1073 K using the DFT-based phonon calculation, are close to the experimental data [10] than the values reported in [14] obtained using QDG approach.

The heat capacity curves calculated using DFT-based phonon and QDG approaches are presented in Figure 8 (b). Both these curves possess a similar attitude of a kink due the same used model [24] describing the ferro/paramagnetic phase transition at T_c. But, at elevated temperatures the curve of heat capacity calculated using QDG approach continues to increase, while the curve calculated using DFT-based phonon approach goes to a horizontal straight line, according to Dulong–Petit law. According to calculations, the former curve will reach a horizontal line at higher temperatures.

The $n8$ is the calculated path of thermal expansion of Fe₂Mo which passing near the experimental values of lattice parameters reported in [10, 12, 13], as shown in Figure 2. The comparison of the free energy calculated along the $n8$ with the energies obtained for other paths calculated in this work using DFT-based phonon calculations and with the energies calculated along the same ni paths using QDG approach reported in [14], can bring us to the conclusion that these two methods used for STEP are equal to each other.

The use of the Debye – Grüneisen method makes it possible to estimate the influence of the vibration energy and the magnetic entropy of local magnetic moments of atoms on the stability of compounds. Whereas in the DFT-based phonon method, the magnetic contribution is already included into the calculations. Thus, it is difficult to evaluate them separately.

This calculation shows that the vibrational energy calculated using phonons differs from the vibrational energy obtained using QDG method, and therefore, if it is used in calculations, taking into account the magnetic entropy is a necessary condition for a correct description of the thermodynamics of compounds containing elements with magnetic properties.

The calculated path of thermal expansion of Fe₂Mo shows that at heating the lattice parameter a - will increase its value while the parameter c - decrease, and vice versa as the temperature decreases. In both

cases, this will cause stresses in the matrix. Therefore, understanding the direction of the thermal expansion path of a compound can help to understand a strengthening mechanism of alloys and in the task of designing new nuclear reactors materials.

4. Conclusions

The first-principles phonon calculations have been carried out to calculate the vibrational energy contribution to the Helmholtz free energy of Fe₂Mo Laves phases. The energetically favourable thermal expansion path of Fe₂Mo was obtained by comparison the free energies calculated along different trajectories of thermal expansion. The obtained results show that the trajectory of thermal expansion path of Fe₂Mo calculated using the quasi-harmonic Debye – Grüneisen approximation closely matches with the path obtained using DFT-based phonon method implemented in this work. Therefore, both of these approaches can equally be used for searching a thermal expansion path. The lattice volume expansion and the isobaric heat capacity were calculated. This study predicts that Fe₂Mo possess a non-isotropic thermal expansion. The results of this work can be used to construct Gibbs potentials to refine the boundaries of the Fe-Mo phase diagram and further design fuel claddings for future nuclear reactors.

Acknowledgments

The research was financially supported by the Russian Foundation for Basic Research as a part of scientific project № 19-03-00530.

References

- [1] V. M. Blinov, Structure and Properties of High-Temperature Austenitic Steels for Superheater Tubes. Russian Metallurgy (Metally), 6 (2009) 478–487. DOI: 10.1134/S0036029509060056
- [2] Y. Hosoi, N. Wade, S. Kunimitsu, T. Urita, Precipitation behavior of laves phase and its effect on toughness of 9Cr-2Mo Ferritic-martensitic steel, Journal of Nuclear Materials, 141-143 (1986) 461-467. [https://doi.org/10.1016/S0022-3115\(86\)80083-6](https://doi.org/10.1016/S0022-3115(86)80083-6).
- [3] Yachun Wang, David M. Frazer, Fabiola Cappia, Fei Teng, Daniel J. Murray, Tiankai Yao, Colin D. Judge, Jason M. Harp, Luca Capriotti, Small-scale mechanical testing and characterization of fuel cladding chemical interaction between HT9 cladding and advanced U-based metallic fuel alloy, Journal of Nuclear Materials, 566 (2022) 153754. <https://doi.org/10.1016/j.jnucmat.2022.153754>.
- [4] R.L. Klueh, K. Shiba, M.A. Sokolov. Embrittlement of irradiated ferritic/martensitic steels in the absence of irradiation hardening J. Nucl. Mater., 377 (3) (2008), pp. 427-437. <https://doi.org/10.1016/j.jnucmat.2008.04.002>
- [5] F.A. Garner, M.B. Toloczko, B.H. Sencer, Comparison of swelling and irradiation creep behavior of fcc-austenitic and bcc-ferritic/martensitic alloys at high neutron exposure, J. Nucl. Mater. 276 (2000) 123. [https://doi.org/10.1016/S0022-3115\(99\)00225-1](https://doi.org/10.1016/S0022-3115(99)00225-1)
- [6] R. Klueh, A.T. Nelson. Ferritic/martensitic steels for next-generation reactors. J. Nucl. Mater., 371 (2007), pp. 37-52. <https://doi.org/10.1016/j.jnucmat.2007.05.005>
- [7] R. Klueh. Elevated temperature ferritic and martensitic steels and their application to future nuclear reactors. Int. Mater. Rev., 50 (2005) 287-310 <https://doi.org/10.1179/174328005X41140>
- [8] V.B. Rajkumar, K.C. Hari Kumar, Thermodynamic modeling of the Fe–Mo system coupled with experiments and ab initio calculations, Journal of Alloys and Compounds 611 (2014) 303-312. <https://doi.org/10.1016/j.jallcom.2014.05.030>
- [9] K. Lejaeghere, S. Cottenier, S. Claessens, M. Waroquier and V. Speybroeck, Assessment of a low-cost protocol for an ab initio based prediction of the mixing enthalpy at elevated temperatures: The Fe-Mo system, Phys. Rev. B 83, (2011) 184201. <https://doi.org/10.1103/PhysRevB.83.184201>
- [10] J. Pavlůa, M. Šob, Ab initio study of C14 Laves phases in Fe-based systems, J. Min. Metall. Sect. B-Metall. 48 (3) B (2012) 395 - 401. [doi: 10.2298/JMMB120704050P](https://doi.org/10.2298/JMMB120704050P)

- [11] D. Vasilyev, Structural, elastic and thermal properties of Laves phase Fe₂Mo from first principles, *J. Phys.: Conf. Ser.* 1942 (2021) 012017. DOI: 10.1088/1742-6596/1942/1/012017
- [12] M. Eumann, G. Sauthoff, M. Palm, Phase equilibria in the Fe–Al–Mo system – Part I: Stability of the Laves phase Fe₂Mo and isothermal section at 800 °C, *Intermetallic* 16 (2008) 706-716.
<https://doi.org/10.1016/j.intermet.2008.02.006>
- [13] X.M. Wang, E.L. Liu, F.C. Yin, X.M. Ouyang, J.X. Hu, Z. Li, W. Qiu, Phase Equilibria of the Fe-Mo-Ta Ternary System, *J. Phase Equilib. and Diffus.* 40 (2019) 413-422.
<https://doi.org/10.1007/s11669-019-00738-8>
- [14] D. Vasilyev, A new method for calculating the thermodynamic and physical properties of compounds: Application to Laves phase Fe₂Mo, *Physica B: Condensed Matter* 621 (2021) 413307,
<https://doi.org/10.1016/j.physb.2021.413307>
- [15] V.I. Moruzzi, J.F. Janak, K. Schwarz, Calculated thermal properties of metals, *Phys. Rev. B* 37 (1988) 790 – 799, <https://doi.org/10.1103/PhysRevB.37.790>.
- [16] F. Körmann, A. Dick, B. Grabowski, B. Hallstedt, T. Hickel, J. Neugebauer, Free energy of bcc iron: integrated ab initio derivation of vibrational, electronic, and magnetic contributions, *Phys. Rev. B*, 78 (2008) 033102, <https://doi.org/10.1103/PhysRevB.78.033102>.
- [17] Y. Wang, L.G. Hector, H. Zhang, S.L. Shang, L.Q. Chen, Z.K. Liu, Thermodynamics of the Ce γ - α transition: density-functional study, *Phys. Rev. B Condens. Matter Mater. Phys.* (2008) 78,
<https://doi.org/10.1103/PhysRevB.78.104113>.
- [18] N. D. Mermin, Thermal Properties of the Inhomogeneous Electron Gas, *Phys. Rev.* (1965) 137,
<https://doi.org/10.1103/PhysRev.137.A1441>.
- [19] L.D. Landau, E.M. Lifshitz. *Statistical physics*. Oxford, New York:Pergamon Press; 1980, 81.
- [20] Y. Wang, Z.-K. Liu, L.-Q. Chen, Thermodynamic properties of Al, Ni, NiAl, and Ni₃Al from first-principles calculations, *Acta Mater.* 52 (2004) 2665-2671,
<https://doi.org/10.1016/j.actamat.2004.02.014>.
- [21] A. van de Walle and G. Ceder, The effect of lattice vibrations on substitutional alloy thermodynamics, *Rev. Mod. Phys.* 74 (2002) 11. <https://doi.org/10.1103/RevModPhys.74.11>
- [22] XiaoYu Chong, Jorge Paz Soldan Palma, Yi Wang, Shun-Li Shang, Fivos Drymiotis, Vilupanur A. Ravi, Kurt E. Star, Jean-Pierre Fleurial, Zi-Kui Liu, Thermodynamic properties of the Yb-Sb system predicted from first-principles calculations, *Acta Materialia*, 217 (2021) 117169.
<https://doi.org/10.1016/j.actamat.2021.117169>.
- [23] Togo A. and Tanaka I., First principles phonon calculations in materials science, *Scr. Mater.*, 108 (2015) 1-5. <http://dx.doi.org/10.1016/j.scriptamat.2015.07.021>
- [24] A.T. Dinsdale, SGTE Data for Pure Elements, *CALPHAD*, 15(4) (1991) 371- 425.
[https://doi.org/10.1016/0364-5916\(91\)90030-N](https://doi.org/10.1016/0364-5916(91)90030-N)
- [25] K. Schwarz, P. Blaha, G.K. Madsen, Electronic structure calculations of solids using the WIEN2k package for material sciences, *Comput. Phys. Commun.* 147 (1–2) (2002) 71-76.
[https://doi.org/10.1016/S0010-4655\(02\)00206-0](https://doi.org/10.1016/S0010-4655(02)00206-0)
- [26] J.P. Perdew, K. Burke, and M. Ernzerhof, Generalized Gradient Approximation Made Simple, *Phys. Rev. Lett.* 77 (1996) 3865. <https://doi.org/10.1103/PhysRevLett.77.3865>
- [27] H.J. Monkhorst and J.D. Pack, Special points for Brillouin-zone integrations, *Phys. Rev. B* 13 (1976) 5188. <https://doi.org/10.1103/PhysRevB.13.5188>
[https://doi.org/10.1016/0364-5916\(82\)90008-6](https://doi.org/10.1016/0364-5916(82)90008-6)
- [28] T.B. Massalski, H. Okamoto, P.R. Subramanian, L. Kacprzak, *Binary Alloy Phase Diagrams* (2nd ed.), ASM International, Materials Park, Ohio, USA, 1990.